Research Square

Preprints are preliminary reports that have not undergone peer review.
They should not be considered conclusive, used to inform clinical practice,
or referenced by the media as validated information.

Sulfotransferase-Mediated Metabolism of Hydroxylated Polychlorinated Biphenyls: Isoform Characterization and Interspecies Differences

xiao-song Li
Nanchang Medical College
Qing feng Chen
Nanchang Medical College
zhong-ze Fang
Tianjin Medical University
Kai Yang
yangkai@ncmc.edu.cn

Nanchang Medical College

Research Article

Keywords: PCBs, OH-PCBs, SULTs, Metabolic characterization

Posted Date: October 22nd, 2026

DOI: https://doi.org/10.21203/rs.3.rs-11251200/v1

License: This work is licensed under a Creative Commons Attribution 4.0 International License.
Read Full License

Additional Declarations: No competing interests reported.

Abstract

Hydroxylated polychlorinated biphenyls (OH-PCBs) are major metabolites of polychlorinated biphenyls (PCBs) and represent important biomarkers of PCB exposure and toxicity in vivo. Phase II conjugation is a major route for the metabolic clearance of OH-PCBs, with sulfation playing an important role in this process. This study aimed to identify the sulfate conjugates of OH-PCBs and characterize the SULT-mediated metabolic pathways in vitro. Using human liver cytosol, monosulfate conjugates were identified as the principal sulfation products. Recombinant enzyme assays showed that SULT1A1, SULT1A2, and SULT1E1 exhibited substantial catalytic activity toward most of the OH-PCB congeners examined. Among these isoforms, SULT1E1 showed the highest catalytic efficiency toward the monochlorinated congeners 4-OH-PCB 2 and 4-OH-PCB 1, whereas SULT1A1 was the most efficient isoform for sulfation of the dichlorinated congener 3'-OH-PCB 9. SULT1A1 made the predominant contribution to the sulfation of the trichlorinated congener 3'-OH-PCB 30; the tetrachlorinated congeners 3'-OH-PCB 65, 4'-OH-PCB 65, 4'-OH-PCB 50, and 4'-OH-PCB 69; and the pentachlorinated congener 4'-OH-PCB 93. Comparative assays using liver cytosol from humans and five animal species revealed congener- and concentration-dependent differences in OH-PCB sulfation, highlighting the need for congener-specific evaluation when extrapolating animal metabolic data to humans. Collectively, these findings provide a systematic characterization of SULT-mediated OH-PCB metabolism and offer new insight into the metabolic clearance and potential toxicological consequences of OH-PCBs in humans.

1. Introduction

Polychlorinated biphenyls (PCBs) are persistent organic pollutants of global concern that were historically used in electrical equipment and various industrial applications (Hamers et al., 2011). Owing to their exceptional chemical stability, PCBs persist in the environment and are widely distributed across environmental matrices, including soil (Tehrani et al., 2014). For example, analysis of 55 surface-soil samples from Shanghai showed PCB concentrations comparable to global background levels (Jiang et al., 2011). Extensive evidence indicates that PCB exposure poses multiple risks to human health. Because of their lipophilicity, PCBs can cross the placenta and have been associated with impaired fetal growth and adverse neurodevelopmental outcomes (Berghuis et al., 2015). PCBs can also disrupt intracellular Ca^{2+} homeostasis and protein kinase C signaling and stimulate reactive oxygen species (ROS) generation, processes implicated in their neurotoxic and pro-oxidative effects (Kodavanti et al., 1995; Brown et al., 1998). In addition, certain PCB congeners inhibit gap-junction intercellular communication, a mechanism that may contribute to tumor-promoting effects (Pencikova et al., 2018).These effects motivate investigation of both parent PCBs and the metabolic processes that determine exposure to their biologically active derivatives.

After entering the human body, PCBs undergo cytochrome P450 (CYP450)-mediated hydroxylation to form OH-PCBs (Tehrani et al., 2014). Compared with their parent compounds, OH-PCBs may exhibit greater biological reactivity and distinct tissue-distribution patterns and are therefore considered important biomarkers of PCB metabolism and toxicity (Grimm et al., 2015).More recently, OH-PCBs have

been identified in postmortem human brain samples, providing further evidence of their occurrence in human tissues (Li et al., 2022). Their subsequent metabolism is therefore relevant to understanding internal exposure to PCB metabolites.Lower-chlorinated OH-PCBs generally have greater water solubility and are more readily metabolized, facilitating renal elimination or further biotransformation (Mills et al., 1985). In contrast, higher-chlorinated OH-PCB congeners retain lipophilic properties similar to those of parent PCBs and may persist in blood and adipose tissues because of their slower elimination (Gallenberg et al., 1990; Guvenius et al., 2003). OH-PCBs can exert multisystem toxicity through several mechanisms. In vitro studies have shown that OH-PCBs induce oxidative stress and apoptosis. For example, OH-PCBs stimulate ROS production in cerebellar granule cells and subsequently trigger cell death (Dreiem et al., 2009). Similarly, 4-OH-PCB 11 induces oxidative stress and ROS generation in human prostate cells, resulting in reduced cell proliferation and viability (Zhu et al., 2013). OH-PCBs can also disrupt reproductive endocrine signaling through interactions with androgen and estrogen receptor pathways (Tam et al., 2022).These observations highlight the need to characterize the conjugation pathways that can alter the availability and biological fate of OH-PCBs.

Sulfation is an important phase II metabolic reaction for numerous xenobiotics, drugs, and endogenous compounds. These reactions are catalyzed by the cytosolic sulfotransferase (SULT) superfamily (Coughtrie, 2016; Falany, 1991). SULT enzymes use 3'-phosphoadenosine-5'-phosphosulfate (PAPS) as the universal sulfate donor and transfer a sulfonate group to hydroxyl or amino groups on acceptor substrates. This conjugation generally increases water solubility and facilitates elimination, often reducing the biological activity of the substrate (Klaassen et al., 1997). For OH-PCBs, the detection of multiple PCB sulfate congeners in serum from mothers and children demonstrates the relevance of sulfation to human PCB metabolism (Zhang et al., 2022). Four SULT families have been identified in humans—SULT1, SULT2, SULT4, and SULT6—comprising at least 13 distinct isoforms (Coughtrie, 2002). SULTs are expressed broadly in both adult and fetal tissues, including the liver, kidneys, lungs, brain, and blood, with the liver exhibiting particularly high expression and sulfation capacity (Riches et al., 2009). Importantly, sulfation does not invariably result in detoxification; some SULT enzymes can bioactivate procarcinogens to reactive electrophiles (Gamage et al., 2006). In the case of PCB metabolites, human hepatic microsomal sulfatase can hydrolyze PCB sulfates to regenerate OH-PCBs, suggesting that sulfation and deconjugation may jointly influence metabolite persistence (Duffel et al., 2021). A recent review further emphasizes the complex roles of sulfation in PCB disposition and toxicity (Duffel and Lehmler, 2024). Thus, identifying the enzymes responsible for sulfate formation is necessary for understanding this pathway, although sulfate formation alone does not establish net elimination.

Recent research has also demonstrated inhibition of human SULT isoforms by OH-PCBs, with inhibitory effects varying among compounds and enzymes (Jia et al., 2021). However, inhibition studies do not by themselves identify the isoforms that metabolize a given OH-PCB or establish their relative contributions to hepatic sulfate formation. Direct comparisons of recombinant SULTs and human liver cytosol, supported by kinetic characterization and chemical inhibition experiments, are needed to address these questions for individual congeners. Because the compounds differ in chlorination pattern and hydroxyl position, their sulfation should be evaluated on a congener-specific basis. Extending these comparisons

to animal liver cytosol at different substrate concentrations can also help determine how closely the tested animal preparations reproduce human sulfation profiles under comparable experimental conditions.

Accordingly, this study aimed to identify the metabolites generated by SULT-catalyzed sulfation of OH-PCBs, determine the major human SULT isoforms responsible for these reactions, and estimate the relative contribution of individual SULT isoforms to OH-PCB metabolism. Nine OH-PCBs spanning mono- to pentachlorinated congeners were examined using human liver cytosol and six recombinant human SULT isoforms. Metabolite identification was combined with apparent kinetic characterization, chemical inhibition experiments, and enzyme abundance-based contribution estimates. In addition, sulfation activities were compared in liver cytosol from humans, monkeys, dogs, rats, pigs, and rabbits at different substrate concentrations. These experiments were designed to clarify congener-dependent sulfation and human SULT involvement and to characterize the interspecies differences relevant to interpreting animal metabolic data.

2. Materials and methods

2.1. Chemicals and reagents

4-OH-3-CB (4-OH-PCB 2), 4-OH-2-CB (4-OH-PCB 1), 3'-OH-2,5-diCB (3'-OH-PCB 9), 3'-OH-2,4,6-triCB (3'-OH-PCB 30), 3'-OH-2,3,5,6-tetraCB (3'-OH-PCB 65), 4'-OH-2,3,5,6-tetraCB (4'-OH-PCB 65), 4'-OH-2,2',4,6-tetraCB (4'-OH-PCB 50), 4'-OH-2,3',4,6-tetraCB (4'-OH-PCB 69), and 4'-OH-2,2',3,5,6-pentaCB (4'-OH-PCB 93) were obtained from J&K Chemical (Beijing, China). Nimesulide, ibuprofen, salbutamol, dehydroepiandrosterone (DHEA), glycyrrhetinic acid (GA), 2,6-dichloro-4-nitrophenol (DCNP), and quercetin were obtained from MedChemExpress (New Jersey, USA). Pooled human liver microsomes from 11 male donors aged 21–38 years and recombinant human SULT isoforms (SULT1A1, SULT1A2, SULT1A3, SULT1B1, SULT1E1, and SULT2A1) were obtained from RILD (Research Institute for Liver Diseases, Shanghai, China). Liver cytosolic fractions from humans, monkeys, dogs, rats, pigs, and rabbits were purchased from Beijing Huizhi Heyuan Biotechnology Co., Ltd. (Beijing, China).Chlorpropamide, dimethyl sulfoxide (DMSO), Brij 58, PAPS, Tris-HCl, and $MgCl_2$ were purchased from Sigma-Aldrich (St. Louis, MO, USA). MS-grade methanol, acetonitrile, and formic acid were purchased from Yirenda Chemical Co., Ltd. (Tianjin, China). Deionized water was produced using a Milli-Q Integral water purification system (Merck KGaA, Shanghai, China).

All OH-PCB stock solutions were prepared in DMSO. Human liver cytosol and recombinant human SULT enzymes were diluted with Tris-HCl buffer. $MgCl_2$ was prepared in deionized water, whereas PAPS, Brij 58, and the specific inhibitors were dissolved in Tris-HCl buffer. Reactions were terminated with ice-cold acetonitrile containing chlorpropamide as the internal standard.

2.2. Analytical instruments and conditions

OH-PCBs and their metabolites were analyzed using an Ekspert ultraLC-100 liquid chromatography system (Eksigent, USA) coupled to a TripleTOF 5600 + mass spectrometer (SCIEX, USA) and a C18 column (2.1 × 100 mm, 1.7 μm; Waters). Mass spectrometric analysis was performed in negative-ion mode. Curtain gas was maintained at 30 psi, and ion source gases GS1 and GS2 were each set to 50 psi. The ion source temperature was 550°C, and the ion spray voltage floating (ISVF) was − 4500 V. For TOF-MS analysis in negative-ion mode, the declustering potential (DP) and collision energy (CE) were set to − 80 V and − 10 V, respectively. For product-ion scans using information-dependent acquisition (IDA), the DP and CE were set to − 80 V and − 45 V, respectively. The scan ranges were m/z 100–800 for TOF-MS and m/z 50–800 for product-ion detection. Chromatographic separation was performed at 40°C using a binary mobile phase consisting of (A) water containing 0.1% formic acid and 10 mM ammonium acetate and (B) acetonitrile/methanol (2:8, v/v), at a flow rate of 0.4 mL/min. The gradient program was as follows: 0–0.5 min, 35% B; 0.5–3 min, 35–60% B; 3–10 min, 60–80% B; and 10–15 min, 35% B, followed by a 2-min re-equilibration period. Metabolite structures were characterized by ultra-performance liquid chromatography coupled with quadrupole time-of-flight mass spectrometry (UPLC/Q-TOF MS). Compound identification and quantification were performed using PeakView 1.2 and MultiQuant 2.1, respectively, based on exact mass (m/z) and chromatographic retention time. Because authentic standards for sulfated OH-PCB metabolites were unavailable, metabolite concentrations in the incubation mixtures were estimated using calibration curves generated with the corresponding parent OH-PCB congeners.

2.3. Sulfation of OH-PCBs in human liver cytosol

Following preliminary optimization of protein concentration (0–0.5 mg/mL) and incubation time (0–120 min), sulfation reactions were performed in a final volume of 200 μL. The incubation mixture contained OH-PCB substrate (0–100 μM), human liver cytosol (0.075 mg/mL), Tris-HCl buffer (50 mM, pH 7.4), $MgCl_2$ (10 mM), Brij 58 (0.5 mg/mg protein), and bovine serum albumin (BSA; 2 mg/mL). The final organic-solvent content did not exceed 1% (v/v). Human liver cytosol was preincubated with Tris-HCl buffer, $MgCl_2$, and Brij 58 on ice for 15 min. After addition of an inhibitor or DMSO as the vehicle control, the mixtures were equilibrated at 37°C in a thermomixer. Reactions were initiated by adding PAPS to a final concentration of 120 μM and incubated with shaking for 40 min. Each reaction was terminated by adding 200 μL of ice-cold acetonitrile containing chlorpropamide as the internal standard. Samples were then centrifuged at 12,500 × g for 10 min, and the supernatants were analyzed by UPLC/Q-TOF MS. Negative controls lacking PAPS, substrate, or human liver cytosol were included to confirm that metabolite formation required both the enzyme source and PAPS. All experiments were performed in duplicate.

2.4. Human SULT isoenzyme phenotyping

The sulfation activities of six commercially available recombinant human SULT isoforms (SULT1A1, SULT1A2, SULT1A3, SULT1B1, SULT1E1, and SULT2A1) were evaluated at low and high substrate concentrations corresponding to approximately 1× and 10× the K_m values determined in human liver cytosol. Reactions were performed at a protein concentration of 0.005 mg/mL under conditions identical

to those used for the human liver cytosol assay, except that Brij 58 was replaced with an equivalent volume of Tris-HCl buffer. After pre-equilibration at 37°C for 5 min, reactions were initiated with 120 μM PAPS and incubated for 40 min. Reactions were terminated with ice-cold acetonitrile containing chlorpropamide as the internal standard. After centrifugation at 12,500 × g for 10 min at 4°C, the supernatants were analyzed by UPLC/Q-TOF MS. Negative controls lacking PAPS, substrate, or the respective SULT isoform were included to confirm enzyme-dependent metabolite formation. All experiments were performed in triplicate.

2.5. Chemical inhibition experiments

The relative contributions of individual SULT isoforms were further evaluated using chemical inhibitors: nimesulide (10 μM; SULT1A1-selective; Pacifici, 2004), ibuprofen (1 mM; SULT1E1-selective; King et al., 2006), quercetin (25 μM) and DCNP (0.5 μM; inhibitors of SULT1A1/1E1; Diao et al., 2014), salbutamol (5 mM; SULT1A3 inhibitor; Ko et al., 2012), and DHEA (30 μM) and GA (30 μM; SULT2A1 inhibitors; Tian et al., 2018). Reaction mixtures were pre-equilibrated at 37°C for 5 min, initiated by addition of 120 μM PAPS, and incubated for 40 min. Reactions were terminated with ice-cold acetonitrile containing chlorpropamide, followed by centrifugation at 12,500 × g for 10 min at 4°C. The resulting supernatants were analyzed by UPLC/Q-TOF MS. All experiments were performed in duplicate.

2.6. Kinetic analysis

Kinetic characterization of OH-PCB sulfation was performed using human liver cytosol and recombinant SULT isoforms. Preliminary experiments confirmed reaction linearity over protein concentrations of 0–0.5 mg/mL and incubation times of 0–120 min. Final incubations contained OH-PCBs at concentrations of 0–1000 μM and either human liver cytosol (0.075 mg/mL) or recombinant SULT enzymes (0.005 mg/mL) and were conducted at 37°C for 40 min. Kinetic data were fitted to the Michaelis-Menten model (Eq. 1) or the substrate-inhibition model (Eq. 2). V_{max} represents the maximum reaction velocity, K_m represents the substrate concentration at half-maximal velocity, and K_i represents the substrate-inhibition constant. All assays were performed in duplicate. Apparent kinetic parameters are reported as mean ± SD and were calculated using GraphPad Prism 8.

$$V = V_{max} \times [S]/(K_m + [S]) \quad (1)$$

$$V = V_{max} \times [S]/(K_m + [S] + [S]^2/Ki) \quad (2)$$

Catalytic efficiency was calculated as V_{max}/K_m.

2.7. Sulfation of OH-PCBs in liver cytosol from different species

Kinetic experiments were conducted using liver cytosol from five non-human species: monkeys, dogs, rats, pigs, and rabbits. OH-PCBs were tested at final concentrations of 0–100 μM and incubated with liver cytosol at a protein concentration of 0.075 mg/mL for 60 min. All other reaction conditions and

procedures were identical to those described above for human liver cytosol. All experiments were performed in duplicate.

3. Results

3.1. Identification of OH-PCB sulfation products in human liver cytosol

UPLC/Q-TOF MS was used to characterize the sulfated metabolites of OH-PCBs. In the human liver cytosol incubation mixture, two major chromatographic peaks were detected (Fig. 1A): the substrate 4-OH-PCB 2 at a retention time of 5.964 min and its sulfated metabolite at 3.789 min. In control incubations lacking PAPS, only the substrate peak was detected (Fig. 1B), confirming that metabolite formation was PAPS dependent. The shorter retention time of the sulfated metabolite is consistent with increased hydrophilicity under reversed-phase chromatographic conditions. The mass spectra of 4-OH-PCB 2 and its sulfated metabolite are shown in Figs. 1C and 1D, respectively. The characteristic isotope patterns arise from the natural abundances of the two stable chlorine isotopes, ^{35}Cl (75.8%) and ^{37}Cl (24.2%) (Zimmermann et al., 2020). In the MS/MS spectrum of the sulfated metabolite (Fig. 1E), a fragment corresponding to a neutral loss of 79.9565 Da was observed, consistent with loss of a sulfonate group. Chromatographic profiles and mass spectra for the remaining OH-PCBs and their sulfated conjugates are shown in Supplemental Figs. 1A–1H, and the corresponding retention times and m/z values are summarized in Table 1.

Table 1
Retention Times and m/z of OH-PCBs and their sulfated conjugates

Compounds	Retention time (min)	m/z
4-OH-PCB 2	5.964	203.0267
Sulfated conjugate	3.789	282.9831
4-OH-PCB 1	5.720	203.0269
Sulfated conjugate	3.872	282.9834
3'-OH-PCB 9	6.631	236.9874
Sulfated conjugate	4.397	316.9436
3'-OH-PCB 30	8.321	270.9489
Sulfated conjugate	5.100	350.9055
3'-OH-PCB 65	9.597	306.9065
Sulfated conjugate	5.745	386.8623
4'-OH-PCB 65	10.405	306.9068
Sulfated conjugate	6.395	386.8626
4'-OH-PCB 50	9.989	306.9065
Sulfated conjugate	6.281	386.8627
4'-OH-PCB 69	10.366	306.9065
Sulfated conjugate	6.315	386.8628
4'-OH-PCB 93	11.125	340.8680
Sulfated conjugate	7.097	420.8245

3.2. Sulfation of OH-PCBs by recombinant SULT enzymes

Kinetic analysis of six recombinant human SULT isoforms revealed marked differences in catalytic activity toward OH-PCBs. For 4-OH-PCB 2 in human liver cytosol (Fig. 2A), the apparent kinetic parameters were V_{max} = 5082 pmol/min/mg protein and K_m = 0.06 μM. Screening at substrate concentrations approximating K_m and 10 × K_m (Fig. 2B) identified SULT1E1 as the most catalytically efficient isoform, whereas no activity was detected for SULT2A1. After normalization to hepatic SULT expression levels (Riches et al., 2009), SULT1A1 accounted for the largest proportion of 4-OH-PCB 2 sulfation at both substrate concentrations (86.81% and 88.25%; Figs. 2C and 2D), whereas SULT1E1 contributed 11.68% and 11.50%, respectively. SULT1A1-mediated sulfation of 4-OH-PCB 2 followed substrate-inhibition kinetics (Fig. 2E). SULT isoform screening and kinetic analyses for the other substrates are presented in Supplemental Figs. 2A–2H. The sulfation reactions were adequately

described by either the Michaelis-Menten or substrate-inhibition model (Table 2). Overall, SULT1E1 showed the greatest catalytic capacity toward the monochlorinated OH-PCBs, whereas SULT1A1 made the predominant contribution to the metabolism of the more highly chlorinated congeners 3'-OH-PCB 30, 3'-OH-PCB 65, 4'-OH-PCB 65, 4'-OH-PCB 50, 4'-OH-PCB 69, and 4'-OH-PCB 93.

Table 2
Apparent kinetic parameters of OH-PCBs sulfonation by HLM and recombinant SULTs

Compounds	Enzyme	Model	K_m(μM)	V_{max}(pmol/min/mg)	K_{si}(μM)	V_{max}/K_m(CL_{int}) (μl/min/mg)
4-OH-PCB 2	HLMs	Substrate inhibition	0.06 ± 0.02	5082 ± 441.4	12.57 ± 3.98	84700.00
	SULT1A1	Substrate inhibition	0.18 ± 0.09	12131 ± 3479	1.36 ± 0.79	67394.44
4-OH-PCB 1	HLMs	Substrate inhibition	0.60 ± 0.35	3478 ± 272.7	81.46 ± 18.54	5796.67
	SULT1A1	Substrate inhibition	1.01 ± 0.27	13173 ± 1545	18.88 ± 4.55	13042.57
3'-OH-PCB 9	HLMs	Substrate inhibition	0.40 ± 0.12	10785 ± 1045	27.43 ± 6.89	26962.50
	SULT1A1	Substrate inhibition	16.81 ± 27.58	490441 ± 713657	1.56 ± 2.53	29175.55
3'-OH-PCB 30	HLMs	Substrate inhibition	4.47 ± 3.18	680.9 ± 258.4	18.87 ± 11.85	152.33
	SULT1A1	Substrate inhibition	0.92 ± 0.26	23829 ± 2180	64.10 ± 17.71	25901.09
3'-OH-PCB 65	HLMs	Substrate inhibition	1.21 ± 0.51	7575 ± 1319	42.42 ± 19.31	6260.33
	SULT1A1	Substrate inhibition	2.96 ± 0.96	235708 ± 24316	380.5 ± 252.8	79631.08
4'-OH-PCB 65	HLMs	Substrate inhibition	3.63 ± 2.22	4835 ± 1376	29.63 ± 15.86	1331.95
	SULT1A1	Substrate inhibition	4.44 ± 2.47	308317 ± 89228	21.11 ± 10.32	69440.77
4'-OH-PCB 50	HLMs	Substrate inhibition	14.79 ± 4.64	4801 ± 992.6	24.34 ± 7.27	324.61
	SULT1A1	Substrate inhibition	4.42 ± 1.52	296876 ± 51511	24.77 ± 7.48	67166.52
4'-OH-PCB 69	HLMs	Substrate inhibition	0.28 ± 0.12	3092 ± 389.2	29.12 ± 10.32	11042.86
	SULT1A1	Substrate inhibition	2.07 ± 1.08	264558 ± 59541	29.74 ± 14.26	127805.80
4'-OH-PCB 93	HLMs	Substrate inhibition	22.20 ± 12.58	9846 ± 3885	29.81 ± 16.91	443.51

Compounds	Enzyme	Model	K_m(μM)	V_{max}(pmol/min/mg)	K_{si}(μM)	V_{max}/K_m(CL_{int}) (μl/min/mg)
	SULT1A1	Substrate inhibition	4.75 ± 1.20	262420 ± 30788	40.06 ± 8.96	55246.52

Chemical inhibition experiments were conducted to further validate the isoform-specific contributions to OH-PCB sulfation in human liver cytosol. The inhibitors included nimesulide (10 μM; SULT1A1), ibuprofen (1 mM; SULT1E1), quercetin (25 μM), DCNP (0.5 μM; SULT1A1/1E1), DHEA (30 μM), and GA (30 μM; SULT2A1). These compounds reduced 4-OH-PCB 2 sulfation by 72.26%, 76.24%, 87.72%, 88.50%, − 0.03%, and 22.32%, respectively (Fig. 2F). The slightly negative inhibition value (− 0.03%) indicates essentially no inhibitory effect. Inhibition patterns for the other OH-PCBs are shown in Supplemental Figs. 2A–2H, and the complete inhibition data are summarized in Table 3.

Table 3
Effects of the selective inhibitors on the formation of metabolites during human liver cytosol incubations

Activity	Inhibition by Nimesulide (SULT1A1)	Inhibition by Ibuprofen (SULT1E1)	Inhibition by Quercetin (1A1 + 1E1)	Inhibition by DCNP (1A1 + 1E1)	Inhibition by DHEA (SULT2A1)	Inhibition by GA (SULT2A1)
4-OH-PCB 2	72.26%	76.24%	87.72%	88.50%	-0.03%	22.32%
4-OH-PCB 1	57.16%	52.99%	93.43%	86.67%	4.23%	13.11%
3'-OH-PCB 9	48.73%	57.31%	94.30%	94.62%	33.34%	-4.67%
3'-OH-PCB 30	73.04%	81.46%	99.04%	92.71%	7.32%	26.97%
3'-OH-PCB 65	60.95%	52.38%	99.06%	88.31%	10.07%	16.39%
4'-OH-PCB 65	58.56%	48.45%	97.04%	79.50%	-6.56%	12.47%
4'-OH-PCB 50	51.52%	40.89%	89.18%	84.20%	2.53%	-11.31%
4'-OH-PCB 69	63.44%	51.80%	94.30%	94.62%	5.75%	0.84%
4'-OH-PCB 93	69.14%	66.63%	84.62%	78.44%	6.63%	-12.10%

Table 4
Enzyme Kinetic Parameters of OH-PCB Sulfation Mediated by liver cytosol Across Species

Compound	Species	Selected model	Km (μM)	Vmax (pmol/min/mg protein)	Vmax/Km (μL/min/mg protein)	Ki (μM)
4-OH-PCB 2	Human	Substrate inhibition	1.447	24010	16590	0.3135
	Monkey	Substrate inhibition	0.1319	3174	24070	33.46
	Dog	Substrate inhibition	0.5499	20770	37770	7.842
	Rat	Michaelis–Menten	1.477	6268	4243	—
	Pig	Substrate inhibition	1.31	11400	8704	55.11
	Rabbit	Substrate inhibition	2.796	22290	7972	5.386
4-OH-PCB 1	Human	Substrate inhibition	1.308	10620	8118	2.266
	Monkey	Substrate inhibition	0.2029	2793	13770	59.01
	Dog	Substrate inhibition	0.303	1640	5413	9.082
	Rat	Substrate inhibition	1.278	1041	814.9	28.09
	Pig	Substrate inhibition	0.3708	801.7	2162	20.19
	Rabbit	Michaelis–Menten	12.42	1626	130.9	—
3'-OH-PCB 9	Human	Substrate inhibition	1.596	58670	36770	0.4117
	Monkey	Substrate inhibition	0.3338	14840	44460	5.412
	Dog	Substrate inhibition	0.4289	25570	59620	6.739
	Rat	Substrate inhibition	5.412	53860	9952	5.306
	Pig	Substrate inhibition	0.2399	5002	20850	8.784

Compound	Species	Selected model	Km (μM)	Vmax (pmol/min/mg protein)	Vmax/Km (μL/min/mg protein)	Ki (μM)
	Rabbit	Substrate inhibition	1.755	92590	52770	5.294
3'-OH-PCB 30	Human	Substrate inhibition	6.024	17290	2871	3.138
	Monkey	Substrate inhibition	1.073	7054	6576	23.59
	Dog	Substrate inhibition	29.58	15330	5181	12.86
	Rat	Substrate inhibition	13.86	21930	1582	90.15
	Pig	Substrate inhibition	1.65	3322	2013	37.1
	Rabbit	Michaelis–Menten	9.825	3234	329.2	—
3'-OH-PCB 65	Human	Substrate inhibition	4.704	74220	15780	0.7662
	Monkey	Substrate inhibition	0.5458	8687	15920	16.37
	Dog	Substrate inhibition	5.208	17410	33430	2.466
	Rat	Substrate inhibition	60.85	11800	193.9	3.53
	Pig	Substrate inhibition	2.592	5967	2302	9.867
	Rabbit	Substrate inhibition	12.82	9360	729.8	22.84
4'-OH-PCB 65	Human	Substrate inhibition	23.62	48710	2062	1.526
	Monkey	Substrate inhibition	0.52	4245	8162	17.58
	Dog	Substrate inhibition	118.6	15970	1346	0.1632
	Rat	Substrate inhibition	40.31	13780	341.9	101.6
	Pig	Substrate inhibition	45.04	5127	113.9	3.575

Compound	Species	Selected model	Km (μM)	Vmax (pmol/min/mg protein)	Vmax/Km (μL/min/mg protein)	Ki (μM)
	Rabbit	Substrate inhibition	75.38	8486	112.6	2.998
4'-OH-PCB 50	Human	Substrate inhibition	7.635	7172	939.4	11.16
	Monkey	Substrate inhibition	4.222	3736	884.9	20.3
	Dog	Substrate inhibition	94.54	83620	884.4	6.951
	Rat	Substrate inhibition	27.29	7705	282.3	168.4
	Pig	Substrate inhibition	94.97	12010	126.5	9.035
	Rabbit	Substrate inhibition	74.32	9711	130.7	5.181
4'-OH-PCB 69	Human	Substrate inhibition	1.822	6143	3371	10.69
	Monkey	Substrate inhibition	0.3575	2638	7379	9.616
	Dog	Substrate inhibition	2.181	33430	15330	6.366
	Rat	Michaelis–Menten	6.091	5749	943.9	—
	Pig	Substrate inhibition	36.13	23600	653.4	33.77
	Rabbit	Substrate inhibition	18.06	49850	2760	319.8
4'-OH-PCB 93	Human	Substrate inhibition	86.25	43690	506.5	3.199
	Monkey	Substrate inhibition	17.02	8435	495.6	5.837
	Dog	Substrate inhibition	52.01	25720	4945	1.006
	Rat	Substrate inhibition	222.4	34480	155	6.248
	Pig	Substrate inhibition	8.855	668.7	75.51	240.5

Compound	Species	Selected model	Km (μM)	Vmax (pmol/min/mg protein)	Vmax/Km (μL/min/mg protein)	Ki (μM)
	Rabbit	Substrate inhibition	16.38	645.6	39.41	368.4

3.3. Sulfation of OH-PCBs in liver cytosol from different species

The available concentration–activity profiles showed congener- and concentration-dependent differences in hepatic cytosolic sulfation among humans, monkeys, dogs, rats, pigs, and rabbits. For 4-OH-PCB 2, the highest observed mean activity occurred at 0.5 μM in both human and monkey cytosol, compared with 1 μM in dog, 5 μM in rabbit, 20 μM in pig, and 80 μM in rat cytosol. In contrast, for 4-OH-PCB 1, human cytosol showed the highest observed maximum among the six species, with its peak at 1 μM; rabbit cytosol reached its maximum at 40 μM. Species differences also varied between positional isomers: at 5 μM, the recorded dog-to-human activity ratio was 5.84 for 3'-OH-PCB 65 but 0.54 for 4'-OH-PCB 65. For 4'-OH-PCB 50, the activity maximum occurred at 5 μM in human and monkey cytosol, 20 μM in pig and rabbit cytosol, and 40 μM in dog and rat cytosol. For 4'-OH-PCB 69, dog cytosol had the highest activity at 5 μM, whereas rabbit cytosol had the highest activity at 40 μM. For 4'-OH-PCB 93, dog cytosol reached its maximum at 5 μM, while human cytosol peaked at 20 μM; the recorded dog-to-human activity ratio at 5 μM was 7.53. Many profiles declined at the upper substrate concentrations.

4. Discussion

OH-PCBs are important metabolites formed during hepatic biotransformation of PCBs and are closely associated with the biological and toxicological effects of PCB exposure. Although the toxic mechanisms of OH-PCBs have been studied extensively, the enzymatic pathways responsible for their further biotransformation and clearance remain incompletely characterized. Clarifying phase II metabolism is therefore important for understanding the elimination kinetics and tissue persistence of OH-PCBs. Previous studies showed that selected OH-PCB isomers can serve as substrates for rat SULT1A1 and SULT2A3 and can be converted to sulfate conjugates (Liu et al., 2009). Sulfated metabolites of hydroxylated 4-chlorobiphenyl were subsequently detected in rat serum and urine (Dhakal et al., 2012), providing in vivo evidence for this metabolic route. Nevertheless, the major human SULT isoforms responsible for OH-PCB sulfation and their relative contributions have remained insufficiently defined.

In the present study, sulfate conjugates of OH-PCBs were identified and their SULT-mediated formation was characterized using human liver cytosol and recombinant human SULT isoforms. OH-PCBs underwent rapid PAPS-dependent sulfation, producing monosulfate conjugates as the major products under the experimental conditions. No metabolite formation was detected in control incubations lacking PAPS, supporting the enzymatic dependence of the reaction. For 4-OH-PCB 2, SULT1A1 made the predominant contribution after normalization to hepatic expression, and the chemical-inhibition

experiment provided additional support: nimesulide reduced sulfation activity by 72.26%, corresponding to 27.74% residual activity. SULT1A1 also made the largest contribution to the sulfation of the more highly chlorinated congeners 3'-OH-PCB 30, 3'-OH-PCB 65, 4'-OH-PCB 65, 4'-OH-PCB 50, 4'-OH-PCB 69, and 4'-OH-PCB 93. Consistent inhibition by nimesulide further supported the involvement of SULT1A1 in these reactions. Kinetic analysis indicated that sulfation of most OH-PCBs by the tested SULT isoforms was best described by a substrate-inhibition model, consistent with the kinetic behavior observed in human liver cytosol.

Interindividual variation in SULT expression or activity may influence the metabolic clearance of OH-PCBs. Reduced sulfation capacity may arise from genetic variation, including single-nucleotide polymorphisms (SNPs) and copy-number variations (CNVs), as well as from physiological or pathological factors that alter SULT expression or activity. Reported examples include lifestyle-related factors such as smoking and alcohol use (Ozbey et al., 2023), acute-phase inflammation (Kim et al., 2004), chronic inflammation (Nilsson et al., 1994), and liver disease, including alcoholic or non-alcoholic cirrhosis and fatty liver disease (Yalcin et al., 2013; Hardwick et al., 2013). These factors may reduce OH-PCB clearance and thereby prolong internal exposure. Consequently, individuals with hepatic dysfunction or functionally relevant SULT polymorphisms may be more susceptible to PCB-associated toxicity and may warrant closer consideration in exposure and risk assessments.

The interspecies comparison suggests that differences in hepatic OH-PCB sulfation depend on both congener structure and substrate concentration. For example, at 5 μM, dog cytosol exhibited higher activity than human cytosol toward 3'-OH-PCB 65 but lower activity toward 4'-OH-PCB 65, indicating that hydroxyl position may influence the relative metabolic activities of different species even when the degree of chlorination is unchanged. This interpretation is supported by the work of Liu, who demonstrated that the substitution patterns of OH-PCBs affected their interactions with rat SULT1A1 and that selected congeners served as substrates, whereas none of the 15 congeners examined were substrates for rat SULT2A3 (Liu et al.,2009). These findings emphasize the importance of isoform-specific substrate recognition when interpreting hepatic sulfation profiles. In addition, Riches identified SULT1A1 as the predominant SULT isoform in human liver, supporting the relevance of enzyme abundance to the substantial contribution of SULT1A1 observed in the present human phenotyping experiments(Riches et a.,2009). Differences in SULT composition, abundance, and substrate recognition could therefore contribute to the interspecies patterns observed here, although these mechanisms require direct investigation in the animal preparations. The concentration-dependent change in the species showing the highest activity toward 4'-OH-PCB 69, from dog at 5 μM to rabbit at 40 μM. Consequently, Selection of an experimental species should instead consider the specific congener and concentration range, with quantitative extrapolation requiring confirmation of comparable assay conditions and validated kinetic parameters.

In conclusion, this study characterized the sulfate conjugates generated during SULT-mediated metabolism of OH-PCBs, identified the principal human SULT isoforms involved, and quantified the relative contributions of individual isoforms to these reactions. The findings define an important phase II

clearance pathway for OH-PCBs and provide a mechanistic basis for understanding how variation in SULT activity may influence human susceptibility to PCB-related toxic effects.

Declarations

Author Contribution

Xiao-song Li: Supervision, Writing – original draft, Conceptualization. Qing-fen Chen: Supervision, Writing – original draft, Conceptualization. Zhong-ze Fang: Writing – review & editing. Kai Yang: Writing – review & editing.

References

1. Berghuis SA, Bos AF, Sauer PJJ, Roze E (2015) Developmental neurotoxicity of persistent organic pollutants: An update on childhood outcome[J]. Arch Toxicol 89(5):687–709
2. Brown AP, Olivero-Verbel J, Holdan WL, Ganey PE (1998) Neutrophil activation by polychlorinated biphenyls: Structure-activity relationship[J]. Toxicol Sci 46(2):308–316
3. Coughtrie MWH (2002) Sulfation through the looking glass—Recent advances in sulfotransferase research for the curious[J]. Pharmacogenomics J 2(5):297–308
4. Coughtrie MWH (2016) Function and organization of the human cytosolic sulfotransferase (SULT) family[J]. Chemico-Biol Interact 259(Pt A):2–7
5. Dhakal K, He X, Lehmler H-J, Teesch LM, Duffel MW, Robertson LW (2012) Identification of sulfated metabolites of 4-chlorobiphenyl (PCB3) in the serum and urine of male rats[J]. Chem Res Toxicol 25(12):2796–2804
6. Diao X, Pang X, Xie C, Guo Z, Zhong D, Chen X (2014) Bioactivation of 3-n-butylphthalide via sulfation of its major metabolite 3-hydroxy-NBP: Mediated mainly by sulfotransferase 1A1[J]. Drug Metab Dispos 42(4):774–781
7. Dreiem A, Rykken S, Lehmler H-J, Robertson LW, Fonnum F (2009) Hydroxylated polychlorinated biphenyls increase reactive oxygen species formation and induce cell death in cultured cerebellar granule cells[J]. Toxicol Appl Pharmcol 240(2):306–313
8. Duffel MW, Lehmler H-J (2024) Complex roles for sulfation in the toxicities of polychlorinated biphenyls[J]. Crit Rev Toxicol 54(2):92–122
9. Duffel MW, Tuttle K, Lehmler H-J, Robertson LW (2021) Human hepatic microsomal sulfatase catalyzes the hydrolysis of polychlorinated biphenyl sulfates: A potential mechanism for retention of hydroxylated PCBs[J]. Environ Toxicol Pharmacol 88:103757
10. Falany CN (1991) Molecular enzymology of human liver cytosolic sulfotransferases[J]. Trends Pharmacol Sci 12(7):255–259
11. Gallenberg LA, Ring BJ, Vodicnik MJ (1990) The influence of time of maternal exposure to 2,4,5,2',4',5'-hexachlorobiphenyl on its accumulation in their nursing offspring[J]. Toxicol Appl

Pharmcol 104(1):1–8

12. Gamage N, Barnett A, Hempel N, Duggleby RG, Windmill KF, Martin JL, McManus ME (2006) Human sulfotransferases and their role in chemical metabolism[J]. Toxicol Sci 90(1):5–22
13. Grimm FA, Hu D, Kania-Korwel I, Lehmler H-J, Ludewig G, Hornbuckle KC, Duffel MW, Bergman Å, Robertson LW (2015) Metabolism and metabolites of polychlorinated biphenyls[J]. Crit Rev Toxicol 45(3):245–272
14. Guvenius DM, Aronsson A, Ekman-Ordeberg G, Bergman A, Norén K (2003) Human prenatal and postnatal exposure to polybrominated diphenyl ethers, polychlorinated biphenyls, polychlorobiphenylols, and pentachlorophenol[J]. Environ Health Perspect 111(9):1235–1241
15. Hamers T, Kamstra JH, Cenijn PH, Pencikova K, Palkova L, Simeckova P, Vondracek J, Andersson PL, Stenberg M, Machala M (2011) In vitro toxicity profiling of ultrapure non-dioxin-like polychlorinated biphenyl congeners and their relative toxic contribution to PCB mixtures in humans[J]. Toxicol Sci 121(1):88–100
16. Hardwick RN, Ferreira DW, More VR, Lake AD, Lu Z, Manautou JE, Slitt AL, Cherrington NJ (2013) Altered UDP-glucuronosyltransferase and sulfotransferase expression and function during progressive stages of human nonalcoholic fatty liver disease[J]. Drug Metab Dispos 41(3):554–561
17. Jia R-Y, Zhang Z-P, Qin G-Q, Zhang W, Yang K, Liu Y-Z, Jiang C, Fang Z-Z (2021) Inhibition of hydroxylated polychlorinated biphenyls (OH-PCBs) on sulfotransferases (SULTs)[J], vol 291. Environmental Pollution, p 118214
18. Jiang Y, Wang X, Zhu K, Wu M, Sheng G, Fu J (2011) Polychlorinated biphenyls contamination in urban soil of Shanghai: Level, compositional profiles and source identification[J]. Chemosphere 83(6):767–773
19. Kim MS, Shigenaga J, Moser A, Grunfeld C, Feingold KR (2004) Suppression of DHEA sulfotransferase (Sult2A1) during the acute-phase response[J]. Am J Physiology-Endocrinology Metabolism 287(4):E731–E738
20. King RS, Ghosh AA, Wu J (2006) Inhibition of human phenol and estrogen sulfotransferase by certain non-steroidal anti-inflammatory agents[J]. Curr Drug Metab 7(7):745–753
21. Klaassen CD, Boles JW (1997) The importance of 3'-phosphoadenosine 5'-phosphosulfate (PAPS) in the regulation of sulfation[J]. FASEB J 11(6):404–418
22. Ko K, Kurogi K, Davidson G, Liu M-Y, Sakakibara Y, Suiko M, Liu M-C (2012) Sulfation of ractopamine and salbutamol by the human cytosolic sulfotransferases[J]. J Biochem 152(3):275–283
23. Kodavanti PRS, Ward TR, McKinney JD, Tilson HA (1995) Increased [^{3}H]phorbol ester binding in rat cerebellar granule cells by polychlorinated biphenyl mixtures and congeners: Structure-activity relationships[J]. Toxicol Appl Pharmcol 130(1):140–148
24. Li X, Hefti MM, Marek RF, Hornbuckle KC, Wang K, Lehmler H-J (2022) Assessment of polychlorinated biphenyls and their hydroxylated metabolites in postmortem human brain samples: Age and brain region differences[J], vol 56. Environmental Science & Technology, pp 9515–9526. 13

25. Liu Y, Smart JT, Song Y, Lehmler H-J, Robertson LW, Duffel MW (2009) Structure-activity relationships for hydroxylated polychlorinated biphenyls as substrates and inhibitors of rat sulfotransferases and modification of these relationships by changes in thiol status[J]. Drug Metab Dispos 37(5):1065–1072
26. Mills RA, Millis CD, Dannan GA, Guengerich FP, Aust SD (1985) Studies on the structure-activity relationships for the metabolism of polybrominated biphenyls by rat liver microsomes[J]. Toxicol Appl Pharmcol 78(1):96–104
27. Nilsson E, de la Torre B, Hedman M, Goobar J, Thörner A (1994) Blood dehydroepiandrosterone sulphate (DHEAS) levels in polymyalgia rheumatica/giant cell arteritis and primary fibromyalgia[J]. Clin Exp Rheumatol 12(4):415–417
28. Ozbey AC, Fowler S, Leys K, Annaert P, Umehara K (2024) Parrott, N. Physiologically-based pharmacokinetic modeling for drugs cleared by non-cytochrome P450 enzymes: State-of-the-art and future perspectives[J]. Drug Metab Dispos 52(1):44–55
29. Pacifici GM (2004) Inhibition of human liver and duodenum sulfotransferases by drugs and dietary chemicals: A review of the literature[J]. Int J Clin Pharmacol Ther 42(9):488–495
30. Pěnčíková K, Svržková L, Strapáčová S, Neča J, Bartoňková I, Dvořák Z, Hýžďalová M, Pivnička J, Pálková L, Lehmler H-J, Li X, Vondráček J (2018) Machala, M. In vitro profiling of toxic effects of prominent environmental lower-chlorinated PCB congeners linked with endocrine disruption and tumor promotion[J]. Environ Pollut 237:473–486
31. Riches Z, Stanley EL, Bloomer JC, Coughtrie MWH (2009) Quantitative evaluation of the expression and activity of five major sulfotransferases (SULTs) in human tissues: The SULT pie[J]. Drug Metab Dispos 37(11):2255–2261
32. Tam N, Lai KP, Kong RYC (2022) Comparative transcriptomic analysis reveals reproductive impairments caused by PCBs and OH-PCBs through the dysregulation of ER and AR signaling[J]. Sci Total Environ 802:149913
33. Tehrani R, Van Aken B (2014) Hydroxylated polychlorinated biphenyls in the environment: Sources, fate, and toxicities[J]. Environ Sci Pollut Res 21(10):6334–6345
34. Tian X, Wang C, Dong P, An Y, Zhao X, Jiang W, Wang G, Hou J, Feng L, Wang Y, Ge G, Huo X, Ning J, Ma X (2018) Arenobufagin is a novel isoform-specific probe for sensing human sulfotransferase 2A1[J]. Acta Pharm Sinica B 8(5):784–794
35. Yalcin EB, More V, Neira KL, Lu ZJ, Cherrington NJ, Slitt AL, King RS (2013) Downregulation of sulfotransferase expression and activity in diseased human livers[J]. Drug Metab Dispos 41(9):1642–1650
36. Zhang D, Saktrakulkla P, Marek RF, Lehmler H-J, Wang K, Thorne PS, Hornbuckle KC, Duffel M (2022) W. PCB sulfates in serum from mothers and children in urban and rural U.S. communities[J], vol 56. Environmental Science & Technology, pp 6537–6547. 10
37. Zhu Y, Mapuskar KA, Marek RF, Xu W, Lehmler H-J, Robertson LW, Hornbuckle KC, Spitz DR (2013) Aykin-Burns, N. A new player in environmentally induced oxidative stress: Polychlorinated biphenyl

congener, 3,3'-dichlorobiphenyl (PCB11)[J]. Toxicol Sci 136(1):39–50

38. Zimmermann J, Halloran LJS, Hunkeler D (2020) Tracking chlorinated contaminants in the subsurface using compound-specific chlorine isotope analysis: A review of principles, current challenges and applications[J]. Chemosphere 244:125476

Figures

Figure 1

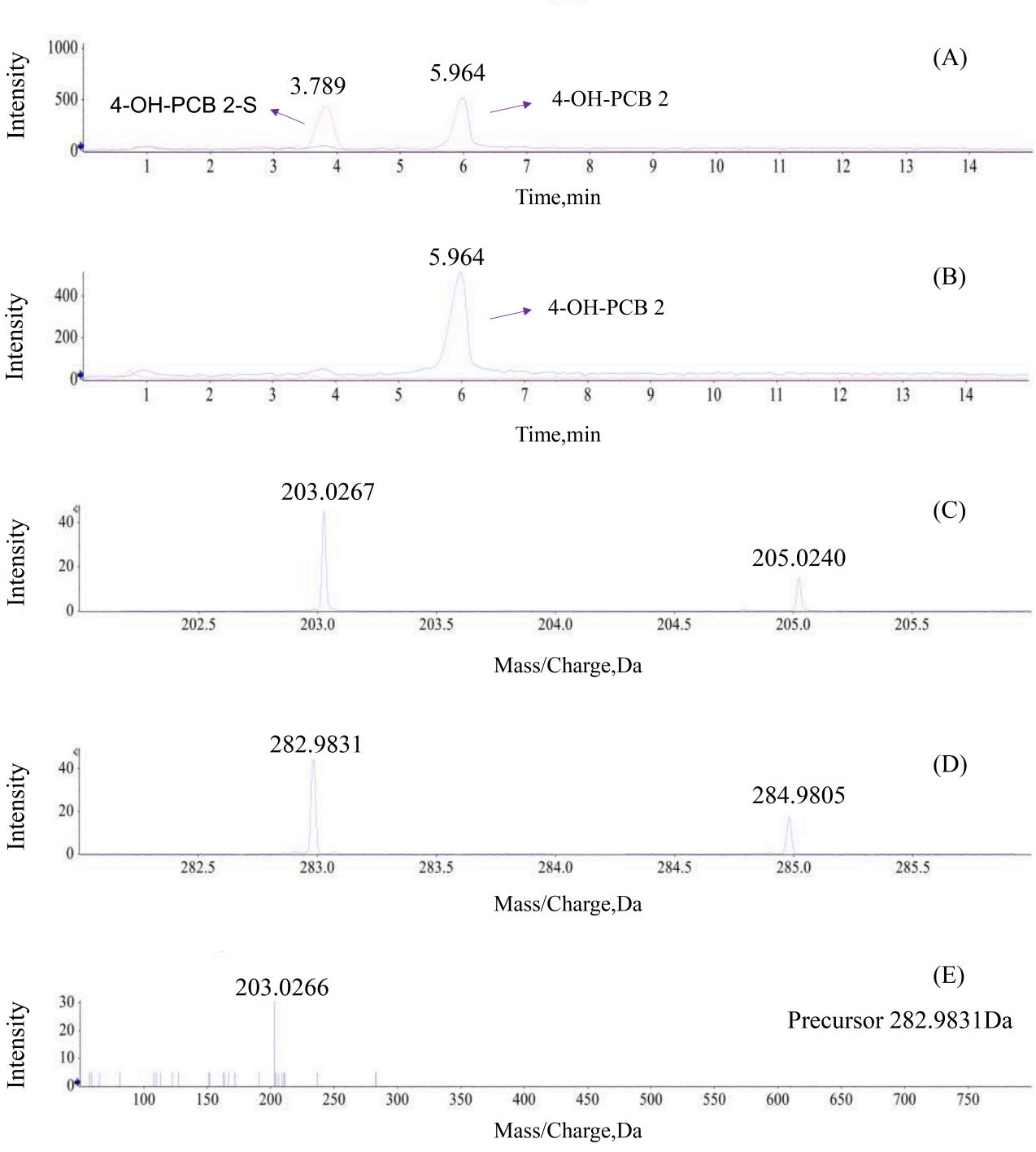

Figure 1

Selected-ion chromatograms of 4-OH-PCB 2 following incubation in human liver cytosol with PAPS (A) or without PAPS (B) for 40 min. Mass spectrum of 4-OH-PCB 2 showing the ion at m/z 203.0267 and its characteristic isotope pattern (C). Mass spectrum of the corresponding sulfate conjugate showing the ion at m/z 282.9831 and its characteristic isotope pattern (D). Product-ion spectrum of the 4-OH-PCB 2 sulfate conjugate (E).

Figure 2

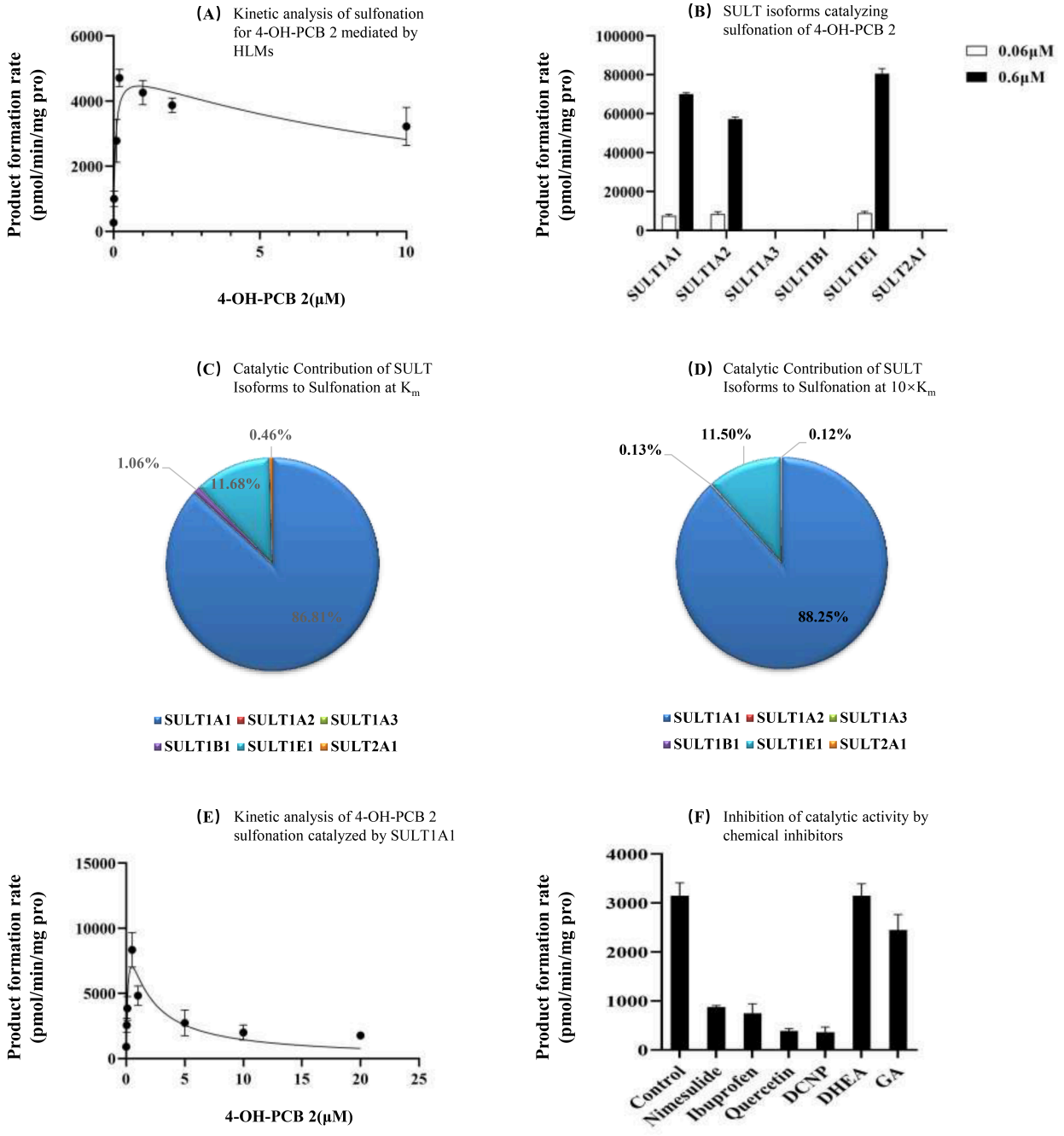

Figure 2

Kinetic analysis of 4-OH-PCB 2 sulfation by human liver cytosol (A) and recombinant SULT1A1 (E); catalytic efficiencies of recombinant SULT isoforms (B); relative metabolic contributions normalized to hepatic SULT expression at 0.06 μM (C) and 0.6 μM (D); and chemical inhibition of 4-OH-PCB 2 sulfation in human liver cytosol by nimesulide (10 μM), ibuprofen (1 mM), quercetin (25 μM), DCNP (0.5 μM), DHEA (30 μM), and GA (30 μM) (F).

Supplementary Files

This is a list of supplementary files associated with this preprint. Click to download.

- SupplementaryInformation.docx
- Graphphoto.png